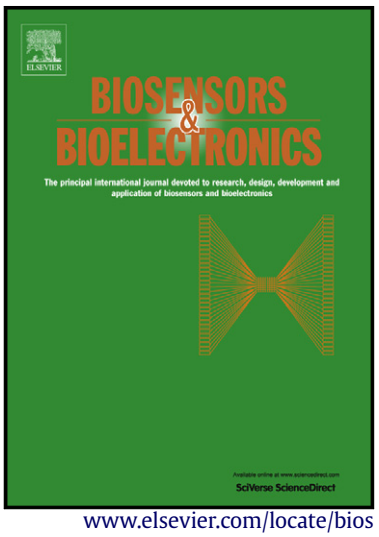

www.elsevier.com/locate/bios

Ordered carbohydrate-derived porous carbons immobilized gold nanoparticles as a new electrode material for electrocatalytical oxidation and determination of nicotinamide adenine dinucleotide

Hadi hosseini, Mohammad Behbahani, Mojtaba Mahyari, Hanif Kazerooni, Akbar Bagheri, Ahmad Shaabani

PII: S0956-5663(14)00134-1
DOI: http://dx.doi.org/10.1016/j.bios.2014.02.046
Reference: BIOS6591

To appear in: *Biosensors and Bioelectronics*

Received date: 8 November 2013
Revised date: 13 February 2014
Accepted date: 15 February 2014

Cite this article as: Hadi hosseini, Mohammad Behbahani, Mojtaba Mahyari, Hanif Kazerooni, Akbar Bagheri, Ahmad Shaabani, Ordered carbohydrate-derived porous carbons immobilized gold nanoparticles as a new electrode material for electrocatalytical oxidation and determination of nicotinamide adenine dinucleotide, *Biosensors and Bioelectronics,* http://dx.doi.org/10.1016/j.bios.2014.02.046

Ordered carbohydrate-derived porous carbons immobilized gold nanoparticles as a new electrode material for electrocatalytical oxidation and determination of nicotinamide adenine dinucleotide

Hadi hosseini, Mohammad Behbahani, Mojtaba Mahyari, Hanif Kazerooni, Akbar Bagheri*, Ahmad Shaabani

Department of Chemistry, Shahid Beheshti University, G. C.; P. O. Box 19396-4716, Tehran, Iran

* Corresponding author. Tel.: +98 21 29903251; fax: +98 21 22431661.

E-mail address: akbr_bagheri@yahoo.com (Akbar Bagheri).

Abstract

The ordered carbohydrate-derived porous carbons (OC-DPCs) were firstly functionalized with thiol groups (−SH) and then immobilized with gold nanoparticles (AuNPs). The Au-SH-OC-DPCs were characterized by CHN analysis, transmission electron microscopy (TEM), fourier transform infrared spectroscopy (FT-IR), X-ray photoelectron spectroscopy (XPS), and x-ray diffraction (XRD). The Au-SH-OC-DPCs were applied for the fabrication of a new electrochemical sensor. The electrocatalytic capabilities of the new sensor were tested by the oxidation of nicotinamide adenine dinucleotide (NADH) in a 0.1 M robinson buffer solution (pH 7.0) using cyclic voltammetry (CV), linear sweep voltammetry (LSV), and differential pulse voltammetry (DPV). The Au-SH-OC-DPCs showed a good voltammetric performance in the electrochemical detection of NADH with a low ~~value of~~ detection limit (1.0 nM), high sensitivity (4.934 μA/μM), and wide linear concentration range (5.0 nM–10 μM).

Keywords: Mesoporous carbon materials; Ordered carbohydrate-derived porous carbons; Gold nanoparticles; Electrochemical biosensor, Nicotinamide adenine dinucleotide.

1. Introduction

An electrochemical biosensor, a subclass of chemical sensors, is an analytical device that converts a biological response into an electrical signal using electrochemical strategies that determine concentrations of substrates and other parameters of biological interest even where no biological system is directly utilized [Bakker and Telting-Diaz, 2002; Chen et al., 2012]. Recently, an intensive research effort has been done in the field of analytical electrochemistry seeking for designs of new electrochemical biosensors capable to provide better analytical characteristics in terms of selectivity, sensitivity, reliability, low cost, and ease of fabrication and use. Nowadays, due to the unique properties of nanomaterials, the use of these materials for the construction of electrochemical biosensor devices constitutes one of the most exciting approaches.

During the past two decades, mesoporous materials (MPM) have attracted enormous attention essentially due to their wide range of applications as molecular sieves, catalysts, separators and gas sensors as well as for electronic and electrochemical devices [Hu et al., 2006].

In the last 10 years, research in these compounds in the field of the electrochemistry has been attracting a great attention mostly with the aim of developing electrocatalysts for diverse applications such as energy conversion devices [Bae et al., 2012; Lang et al., 2011; Li et al., 2007; Shin and Lee, 2008] (e.g. fuel cell, battery, supercapacitor, solar cell), and sensor fabrication [Hosseini et al., 2013; Hu et al., 2008; Wang et al., 2013]. Mesoporous carbon materials (MPCM) are one of the major porous materials which used extensively as electrode materials for batteries, fuel cells, and supercapacitors. The MPCMs can be used also as sorbents for the separation processes, gas storage, and as supports for many important catalytic processes [Liang et al., 2008]. Their use in such diverse applications is related not only to their unique

physical and chemical properties, such as electric conductivity, thermal conductivity, chemical stability, and high specific surface areas~~, high order and high ability to modified in countless ways, and low density,~~ but also to their wide availability [Lee et al., 2006; Liang et al., 2008]. The ordered carbohydrate-derived porous carbons (OC-DPCs) are one of the newest MPCM which recently have been synthesized using renewable materials (environmentally friendly method) by Kubo et al. [Kubo et al., 2011]. The OC-DPCs synthesized through a sugar-based direct hydrothermal carbonization (HTC)/soft-templating approach in which D-Fructose functioned as a carbon precursor whereas Pluronic F127 acted as a pore template during the synthesis under hydrothermal conditions. The OC-DPCs synthesized by this method have unique properties such as having well defined ordered mesoporous domains, high specific surface areas, and good thermal and chemical stability. The unique properties of OC-DPCs make them potential candidates for various applications including adsorption, separation ~~science~~, catalysis, and more recently in the area of new energy cycles (e.g., electrochemistry, energy storage, and fuel cells).

Metal nanoparticles, especially gold nanoparticles (AuNPs), have received great interests due to their attractive optical, electronic, and thermal properties as well as catalytic properties and potential applications in the fields of chemistry, biology, medicine, physics, and material science ~~and their different interdisciplinary fields~~ [Guo and Wang, 2007; Rashid et al., 2006]. In the field of electrochemistry, the excellent conductivity and catalytic properties of AuNPs make them suitable for acting as “electronic wires”. The use of AuNPs as an electrode enhances the electron transfer between redox centers and electrode surfaces and also acts as catalysts for electrochemical reactions [Luo et al., 2006; Saha et al., 2012]. These attractive properties of AuNPs make them extremely suitable for designing new and improved electrochemical sensing

devices, especially sensors and biosensors. Furthermore, control over the size, shape, stability, and surface chemistry of AuNPs create novel catalytic properties for AuNPs such as a high surface-to-volume ratio, high surface energy, and facilitate electron transfer between redox centers and electrode surfaces. These properties are remarkably different from those of the corresponding bulk materials and also tunable by changing parameters affecting NPs structures [Hu and Dong, 2008]. As an outcome, the development of methods that allow control of NPs size, shape, stability and dispersity is a major subject for research. One of the important ways to achieve this control is immobilization and stabilization of the nanoparticles on the supporting materials such as graphene, conductive polymers and carbon nanotubes [Hu and Dong, 2008; Ge et al., 2012; Georgakilas et al., 2012; Pingarrón et al., 2008]. Nowadays, due to the unique physical and chemical properties of MPCM, the immobilization and stabilization of the nanoparticles on their surface are ~~have~~ attractive in various fields including medicine, catalysis and sensors [White et al., 2009]. Similar to MPCM, OC-DPCs due to their excellent properties such as high porosity and surface area can be an ideal candidate for the immobilization and stabilization of nanoparticles. Thus, combining the unique properties of OC-DPCs and electrocatalytic properties of metal NPs could open up a new range of applications for these materials and could introduce a new way into the electrode surface modification for designing new electrochemical sensors. Moreover, Due to their specific structure and the existence of hydroxyl functional groups, it is possible to functionalize OC-DPCs using either covalent or noncovalent chemistry in order to obtain excellent nanoparticle supporters with intrinsic properties.

Nicotinamide adenine dinucleotide (NADH) is involved as a cofactor in several hundred enzymatic reactions of NAD^+/NADH dependent dehydrogenases [Bergel et al., 1989; Saleh et al.

2011]. The electrochemical oxidation of NADH is of great interest [Chen et al., 2013; Sun et al., 2013; Teymourian et al., 2013; Zhang et al., 2014] because of its significance as a cofactor for dehydrogenase enzymes and its role in the electron-transfer chain in biological systems. Therefore, the development of electrochemical biosensors for detection of NADH is vital [Shan et al., 2010]. The catalytic ability of AuNPs for oxidation of NADH has been widely studied [Chang et al., 2011; Jena and Raj, 2006; Raj and Jena, 2005; Zhang and Oyama, 2007]. Based on the above mentioned preface, in this work, we were inspired to explore the integration of OC-DPCs with AuNPs for the electrocatalytic oxidation and determination of NADH. To better immobilization and interaction of AuNPs, the OC-DPCs were functionalized with thiol groups (−SH). This is the first example of a highly active porous-OC-DPCs-supported AuNPs catalyst for the electrochemical oxidation of NADH.

2. Experimental

2.1. Materials

All reagents include solvents, acids, 3-thiol-propyltriethoxysilane and D-Fructose were of analytical grade and purchased from Merck Company (Darmstadt, Germany). NADH (disodium salt, 98%) was obtained from Sigma. Pluronic® F127 triblock (Mw = 12600, EO106-PO70-EO106) copolymer was purchased from Aldrich Company. Double-distilled water from a Milli-Q purification system (Millipore, Bedford, MA, USA) was used for the preparation of solutions.

2.2. Apparatus

Electrochemical studies were carried out in a glass cell incorporating three electrodes configuration containing 20 mL of 0.1 M robinson buffer solution as ~~running~~ electrolyte using the ~~powered by~~ μ-Autolab type III. The working electrode, counter electrode and reference

electrode used in the voltammetry experiments were a modified glassy carbon electrode, a platinum wire and Ag/AgCl, respectively. The pH was measured at 25 ± 1 ºC with a digital WTW Metrohm 827 Ion analyzer (Herisau, Switzerland) equipped with a combined glass-Calomel electrode. The CHN analysis was performed on a Thermo Finnigan Flash EA112 elemental analyzer (Okehampton, UK). N_2 adsorption surface areas were measured by BET technique using a Micrometritics ASPS 2010 analyzer. IR spectra were recorded on a Bruker IFS-66 FT-IR Spectrophotometer. Low-angle X-ray diffraction patterns were obtained on a Philips-PW 17C diffractometer with Cu K_α radiation. Thermogravimetry and differential scanning calorimetry (TG/DTA) was carried out on a Bahr STA-503 instrument under air atmosphere. The TEM micrograph was recorded by a Philips EM420 transmission electron microscope.

2.3. Preparation of Ordered carbohydrate-derived porous carbons (OC-DPCs)

The *OC-DPCs* were synthesized according to the recently reported procedure using D-Fructose (Fru) as a carbon source [Kubo et al., 2011]. In this approach, 0.25 g of Plorunic F127 and 1.20 g of Fructose were dissolved in 10 mL of deionized water and then solution was transferred to a Teflon lined sealed steel autoclave and placed at 130 °C for 3 days. ~~Then~~ The dark-brown solid precipitate was obtained and washed with water and ethanol. After that the prepared compound was dried at room temperature. The calcination was performed under nitrogen atmosphere at 550 ^{o}C for 6 h. The synthesis of mesoporous carbons was confirmed by X-ray powder diffraction and also nitrogen adsorption analysis.

2.4. Preparation of thiol functionalized ordered carbohydrate-derived porous carbons (SH-OC-DPCs)

In this approach~~, in a typical reaction~~, 1.0 g of *OC-DPCs* was suspended in 50 mL of toluene~~,~~ and 2 mL of 3-thiol-propyltriethoxysilane ~~(2.0 mL)~~ was added to the mixture ~~and~~ which was refluxed for 48 h under nitrogen atmosphere. ~~Then~~ The prepared black solid was removed from solvent by filtration, washed with methanol and acetone and then dried at room temperature.

2.5. Preparation of Au nanoparticles supported on thiol ordered carbohydrate-derived porous carbons (Au-SH-OC-DPCs)

Aqueous solution of $HAuCl_4$ (0.2 g in 3.0 mL) and SH-*OC-DPCs* (0.2 g in 10.0 mL) were mixed and placed in an ultrasonic bath (50 KHz) for 30 min to well disperse metal ions in the *SH-OC-DPCs*. Then 10.5 mL of a 1.0 M $NaBH_4$ solution in 0.3 M aqueous NaOH was added to mixture for the reduction process and form gold nanoparticles. After stirring for 4 h, it was filtered under vacuum, washed well with ethanol and water and dried under vacuum at 50 °C for 12 h.

2.6. *Preparation of the modified glassy carbon electrodes*

Prior to the electrode modification process, a well polished 2mm in diameter glassy carbon electrode (polishing was performed with 0.05 μm alumina slurry on a polishing cloth) was washed with deionized water and ethanol. ~~after~~ ~~Typically~~ A stable suspension solution containing 1.0 mg ml^{-1} of Au-SH-OC-DPCs in DMF was prepared by using 20 min ultrasonic agitation. After the electrode surface was air dried, 10.0 μL of this suspension was casted onto the surface of the pretreated GC electrode with a microsyringe and then ~~it was~~ dried in air. ~~Furthermore,~~ Also, the suspension of OC-DPCs was prepared and used with the same procedure.

3. Results and discussion

3.1. Characterization of prepared catalysts

Fig 1 shows the TEM images of (A) SH-OC-DPCs and (B) Au-SH-OC-DPCs, representing the uniformly dispersed and the size distribution of supported gold nanoparticles on the carbon nonporous. Moreover, TEM analysis indicates that nanoparticles are in the range of 5-7 nm.

Fig. 2 shows the XPS survey data of Au-SH-OC-DPCs, indicating the binding energy (BE) of different atoms (Au, Si, S, C, and O). The BEs at around 84.1, 103.4, 162.3, 286.3, and 532 can be assigned ~~due~~ to the presence of Au(4f), Si(2p), S(2p), C(1s), and O(1s) elements, respectively. Additional information about the characterization of prepared catalysts is described in supplementary data.

Here Fig. 1

Here Fig. 2

3.2. Electrochemistry of NADH at Au-SH-OC-DPCs

To address the analytical applicability of the Au-SH-OC-DPCs/GCE, The electrocatalysis ability of the Au-SH-OC-DPCs/GCE was evaluated for the electrooxidation of NADH. At first, the electrochemistry of NADH on the surface of different modified electrodes was studied using cyclic voltammetry (CV). Fig. 3A depicts the typical CV curves of 1.0 μM NADH at GCE, OC-DPCs/GCE and Au-SH-OC-DPCs/GCE in a 0.1 M robinson buffer solution pH 7.0 at 50 mV/s scan rate. In this condition, no peak is observed for the electrochemical oxidation of NADH on both GCE and OC-DPCs/GCE surfaces. When the electrode surface was modified with the Au-SH-OC-DPCs, the CV response of Au-SH-OC-DPCs/GCE electrode in the 0.1 M robinson buffer solution pH 7.0 in the absence of NADH show one anodic peak which was started to appear between + 0.75 V to 1.5 V during the anodic scan, corresponding to electrochemical

oxidation of AuNPs to Au oxide species. Upon scanning to cathodic direction, a new peak started to appear approximately at 0.46 V which it may be related to the reduction of Au oxide species generated in the anodic scan [Hosseini et al., 2013; Burke et al., 2003].

Here Fig. 3

The CV curve of Au-SH-OC-DPCs/GCE in the presence of 1.0 μM NADH shows the electro-catalytic activity for NADH oxidation. As seen from Fig. 3A, a well-defined anodic peak was appeared at 0.9 V in the positive scan rate which its current peak is higher than that of AuNPs oxidation, As well as, in the negative scan rate, a cathodic peak was appeared approximately at 0.50 V which its current is lower than that of the reduction of Au oxide species. It seems that the mechanism of the electrocatalytic activity of Au-SH-OC-DPCs/GCE toward NADH oxidation is based on the hypothesis that Au-sites are active sites for the oxidative dehydrogenation (ODH) of NADH to NAD^+. At first, the AuNPs were oxidized to Au oxide (AuOx) form, these surface oxides apparently exist at the interface as either AuOH or $Au(OH)_3$, and these oxide species are considered as mediators for the oxidation of NADH. The interactions of NADH with the AuOxNPs can promote the C–H bond rupture which it is necessary for NADH oxidation [Xing et al., 1996; Thompson, 1999]. Therefore, the electrochemical oxidation of NADH can be explained as follow (Scheme 1):

Here Scheme 1

~~Furthermore, with~~ By increasing the NADH concentration (Fig. 3B), the intensity of cathodic peak decreased. These results indicated that with the increasing NADH concentrations, more surface Au oxides were used for NADH oxidation. In addition, NADH undergoes oxidation at

unusually–high potential, which this is a complicated behavior and it can be assigned to the electrochemical oxidation of AuNPs to Au oxide species at relatively high potentials.

The effect of pH on the anodic response of NADH was tested by recording the CVs of 1.0 μM NADH at Au-SH-OC-DPCs/GCE in 0.1 M robinson buffer solution from pH 2.0–8.0 at a scan rate of 50 mV/s. Within this pH range, the maximum peak current was observed at pH 3.0. However, in order to mimic the physiological condition, pH 7.0 was chosen in this study.

The effect of potential scan rate on the electrochemical behavior of NADH oxidation at the Au-SH-OC-DPCs/GCE electrode was investigated at ranges from 25.0 to 250.0 mV/s by linear sweep voltammetry (LSV). As it can be seen (Fig. 4A), the peak current associated to the NADH electro-oxidation increases linearly with the square root of scan rate, which indicates that the electrocatalytic process under study is controlled by diffusion.

Here Fig. 4

~~Furthermore,~~ By increasing the scan rate, the peak potential shifts to more positive values. This behavior was expected for an irreversible electrode process (Fig. 4B). For a diffusion-controlled and irreversible electrode process, according to Brett and Brett (Wang et al., 2009), the relationship between the peak potential (Ep) and scan rate (υ) is defined as following (Bard and Faulkner, 2001):

$$\left| dEp/d \log \upsilon^{1/2} \right| = 0.0592/(1-\alpha n') \qquad (1)$$

The value of (αn′) can be easily estimated from the slope of Ep vs. log $\upsilon^{1/2}$. In our system, the slope is 0.088. Generally, n′ is assumed (Bard and Faulkner, 2001) to be 1.0 in the rate determining step. Thus, α was calculated to be 0.33.

3.3. Electrochemical determination of NADH at Au-SH-OC-DPCs

~~As~~ Differential-pulse voltammetry (DPV) is one of the most sensitive electrochemical detection methods~~,~~ and it was used in this study for the quantitative analysis of NADH. Fig. 5A shows some DPV curves of NADH at different concentrations using the Au-SH-OC-DPCs/GCE. Well-defined voltammograms were obtained. The peak current increased linearly with increment of NADH concentrations in the range from 5.0 nM to 10 μM (Fig. 5B). The linear regression equations were I_{pa} (μA) = 4.934 C_{NADH} (μM) + 0.563, with a correlation coefficient of 0.999, a high sensitivity of 4.934 μA/μM and a limit of detection (LOD) of 1.0 nM. The main advantages of the Au-SH-OC-DPCs/GCE are good analytical performances such as low detection limit, wide linear range, and high sensitivity. ~~and~~ To the best of our knowledge, this is the lowest concentration value ever reported for the NADH determination on the electrodes. Therefore, the sensor can be used to readily detect NADH in the low range levels with a good sensitivity. The analytical performances of the proposed method were compared with commercial method (El-Ansary and Faddah, 2010). In this method, the NADH was analyzed using spectroscopic method which has a higher LOD (0.45 μM) compared to our proposed method. The characteristics of the new sensor for NADH determination are summarized in Table 1 and the data is compared to the partial sensors. The results demonstrate that the new sensor features a lower detection limit compared to the other ones.

Here Table 1

To characterize the reproducibility of the electrode, ten repetitive measurements were carried out for 0.01 and 1 μM NADH solutions. The Au-SH-OC-DPCs/GCE surface renewal gives a good reproducible surface since the relative standard deviations obtained were 2.02 and 2.67%, respectively. In addition, one of the advantages with this electrode is that the rapid decay of the signal was not observed and the electrode does not undergo surface fouling during the

measurements. Furthermore, the electrochemical activity of the Au-SH-OC-DPCs/GCE remained 97% and 95% after 24 and 48h storage in the doubly distilled water, respectively, and remained 96% after one week storage in the air, suggesting that the stability of the electrode was good.

Here Fig. 5

Some inorganic ions and organic compounds which coexist with NADH in biological samples, can affect the voltammetric response of this compound. Thus, the effect of potentially interfering substances such as Zn^{2+}, Na^{+}, K^{+}, Mg^{2+}, Ca^{2+}, Fe^{3+}, SO_4^{2-}, Cl^{-}, nitrate, fructose, sucrose, talc, citric acid, ascorbic acid, and uric acid on the voltammetric response of NADH were investigated by using DPV. The results showed that no interference was observed on the signals of NADH in the presence of 100 fold interfering substances to NADH concentrations. Some results for NADH are presented in Table 1S.

4. Conclusion

We have prepared the SH-OC-DPCs immobilized with AuNPs for the fabrication of electrochemical sensors and was characterized ~~it~~ by TEM, XPS, XRD, and CHN analysis. The oxidation of NADH was used to test the electrocatalytic capabilities of Au-SH-OC-DPCs electrode using CV, LSV, and DPV. The electrocatalytic current increased linearly with the NADH concentration in the range of 5.0 nM–10 μM with a slope of 4.934 μA/μM and detection limit of 1.0 nM.

References

Bae, J.H., Han, J.-H., Chung, T.D., 2012. Phys. Chem. Chem. Phys. 14, 448–463.

Bakker, E., Telting-Diaz, M., 2002. Anal. Chem. 74, 2781–2800.

Bard, A.J., Faulkner, L.R., 2001. Electrochemical Methods: Fundamentals and Applications, Wiley, New York.

Bergel, A., Souppe, J., Comtat, M., 1989. Anal. Biochem. 179, 382–388.

Burke, L.D., Moran, J.M., Nugent, P.F., 2003. J. Solid State Electrohem. 7, 529-538.

Chang, H., Wu, X., Wu, C., Chen, Y., Jiang, H., Wang, X., 2011. Analyst 136, 2735-2740.

Chen, C.-H., Chen, Y.-C., Lin, M.-S., 2013. Biosens. Bioelectron. 42, 379-384.

Chen, D., Feng, H., Li, J., 2012. Chem. Rev. 112, 6027−6053.

El-Ansary, A., Faddah, L.M., 2010. Nanotech. Sci. App. 3, 65–76.

Ge, S., Yan, M., Lu, J., Zhang, M., Yu, F., Yu, J., Song, X., Yu, S., 2012. Biosens. Bioelectron. 31, 49– 54.

Georgakilas, V., Otyepka, M., Bourlinos, A.B., Chandra, V., Kim, N., Kemp, K.C., Hobza, P., Zboril, R., Kim, K.S., 2012. Chem. Rev. 112, 6156−6214.

Guo, S., Wang, E., 2007. Anal. Chim. Acta 598, 181–192.

Hosseini, H., Ahmar, H., Dehghani, A., Bagheri, A., Fakhari, A.R., Amini, M.M., 2013. Electrochim. Acta 88, 301– 309.

Hu, K., Lan, D., Li, X., Zhang, S., 2008. Anal. Chem. 80, 9124–9130.

Hu, X., Dong, S., 2008. J. Mater. Chem. 18, 1279–1295.

Hu, Y.-S., Guo, Y.-G., Sigle, W., Hore, S., Balaya, P., 2006. J. Maier, Nat. Mater. 5, 713-717.

Jena, B.K., Raj, C.R., 2006. Anal, Chem, 78, 6332-6339.

Kubo, S., White, R.J., Yoshizawa, N., Antonietti, M., Titirici, M.-M., 2011. Chem. Mater. 23, 4882−4885.

Lang, X., Hirata, A., Fujita, T., Chen, M., 2011. Nat. Nanotech. 6, 232–236.

Lee, B.J., Kim, J., Hyeon, T., 2006. Adv. Mater. 18, 2073–2094.

Li, H., Bian, Z., Zhu, J., Huo, Y., Li, H., Lu, Y., 2007. J. Am. Chem.Soc. 129, 4538–4539.

Liang, C., Li, Z., Dai, S., 2008. Angew. Chem. Int. Ed. 47, 3696 – 3717. [6] Shin, Y., Lee, S., 2008. Nano Lett. 8, 3171–3173.

Luo, X., Morrin, A., Killard, A.J., Smyth, M.R., 2006. Electroanalysis 18, 319–326.

Manesh, K.M., Santhosh, P., Gopalan, A., Lee, K.P., 2008. Talanta 75, 1307–1314.

Thompson, D., 1999. Gold Bulletin 32, 12-19.

Pingarrón, J.M., Yáñez-Sedeño, P., González-Cortés, A., 2008. Electrochimica Acta 53, 5848–5866.

Prasad, K.S., Chen, J.-C., Ay, C., Zen, J.-M., 2007. Sens. Actuat. B 123, 715–719.

Raj, C.R., Jena, B.K., 2005. Chem. Commun. 2005-2007.

Rao, T.N., Yagi, I., Miwa, T., Tryk, D.A., Fujishima, A., 1999. Anal. Chem. 71, 2506-2511.

Rashid, M.H., Bhattacharjee, R.R., Kotal, A., Mandal, T.K., 2006. Langmuir 22, 7141–7143.

Saha, K., Agasti, S.S., Kim, C., Li, X., Rotello, V.M., 2012. Chem. Rev. 112, 2739−2779.

Saleh, F.S., Rahman, M.R., Okajima, T., Mao, L., Ohsaka, T., 2011. Bioelectrochemistry 80(2), 121-127.

Shan, C., Yang, H., Han, D., Zhang, Q., Ivaska, A., Niu, L., 2010. Biosens. Bioelectron. 25, 1504–1508.

Sharifi, E., Salimi, A., Shams, E., 2013. Biosens. Bioelectron. 45, 260-266.

Stergiou, D.V., Prodromidis, M.I., Veltsistas, P.G., Evmiridis, N.P., 2004. Electroanal. 16, 949-954.

Sun, Y., Ren, Q., Liu, X., Zhao, S., Qin, Y., 2013. Biosens. Bioelectron. 39, 289-295.

Teymourian, H., Salimi, A., Khezrian, S., 2013. Biosens. Bioelectron. 49, 1-8.

Wang, Y., Wu, B., Gao, Y., Tang, Y., Lu, T., Xing, W., Liu, C., 2009. J. Power Sources 192, 372-375.

Wang, Y., Wu, Y., Xie, J., Hu, X., 2013. Sens. Actuat. B: Chemical 177, 1161-1166.

White, R.J., Luque, R., Budarin, V.L., Clark, J.H., Macquarrie, D.J., 2009. Chem. Soc. Rev. 38, 481–494.

Xing, X., Shao, M., Liu, C.-C., 1996. J. Electroanal. Chem. 406, 83-90.

Zare, H.R., Nasirizadeh, N., Mazloum-Ardakani, M., Namazian, M., 2006. Sens. Actuat. B 120, 288–294.

Zhang, Y., Bo, X., Nsabimana, A., Luhana, C., Wang, G., Wang, H., Li, M., Guo, L., 2014. Biosens. Bioelectron. 53, 250-256.

Zhang, J., Oyama, M., 2007. Electrochem. Commun. 9, 459-464.

Table, figure and scheme captions:

Table 1. Comparison of analytical characteristics of Au-SH-OC-DPCs toward the NADH oxidation with some reported electrodes.

Scheme 1. Electrochemical oxidation of NADH on the surface of Au-SH-OC-DPCs/GCE

Fig. 1. The TEM images of (A) SH-OC-DPCs and (B) Au-SH-OC-DPCs.

Fig. 2. Wide XPS scan of Au-SH-OC-DPCs.

Fig. 3. (A): CV curves of the GCE, OC-DPCs/GCE, and Au-SH-OC-DPCs/GCE in a 0.1 M robinson buffer solution pH 7.0 with (blue lines) and without (black lines) 1.0 μM NADH. Scan rate: 50 mV/s. **(B):** CV curves of NADH at Au-SH-OC-DPCs/GCE in a 0.1 M robinson buffer solution pH 7.0 at 50 mV/s scan rate: NADH concentrations (from a to d): 0.05, 0.1, 0.5, and1.0 μM. Black lines are CV curve of electrodes in the absence of NADH.

Fig. 4. (A): plot of the peak current with square root of scan rate. (B): plot of the variation of peak potential with logarithm of the square root of scan rate.

Fig. 5. (A): DPVs of Au-SH-OC-DPCs/GCE in 0.1 M robinson buffer solution pH 7.0 at different concentrations of NADH: 0.01, 0.1, 0.2, 0.3, 0.5, 1.0 and 2.0 μM of NADH (from a to g). **(B):** linear calibration curves of the DPVs currents vs. NADH concentrations.

Table 1

Electrode Materials	Linear ranges	LOD	RSD (μA/μM)	Ref.
PEDOT–PSS-Au_{nano}[a]	1–80 μM	0.1 μM	----	Manesh et al., 2008
SPCE[b]	----	157nM	----	Prasad et al., 2007
HMCPE[c]	0.4–10.0 μM	0.08 μM	0.0028 μA/μM	Zare et al., 2006
DB1-CME[d]	0.002 to 0.1 mM	0.002 mM	----	Stergiou et al., 2004
IL-G[e]	0.25 to 2mM	----	----	Shana et al., 2010
NiOxNPs[f]	0.3 μM to 1 mM	106 nM	----	Sharifi et al., 2013
BDD[g]	10-500 nM	10 nM	----	Rao et al., 1999
Au-SH-OC-DPCs	5.0 nM–10 μM	1.0 nM	4.934 μA/μM	This work

[a] Gold nanoparticles loaded poly(3,4-ethylenedioxythiophene)–poly(styrene sulfonic acid)

[b] Screen printed carbon electrode

[c]Hematoxylin modified carbon paste electrode

[d]Disperse Blue 1-chemically modified electrodes

[e]Ionic liquid-functionalized graphene

[f]nickel oxide nanoparticles

[g]Boron-Doped Diamond

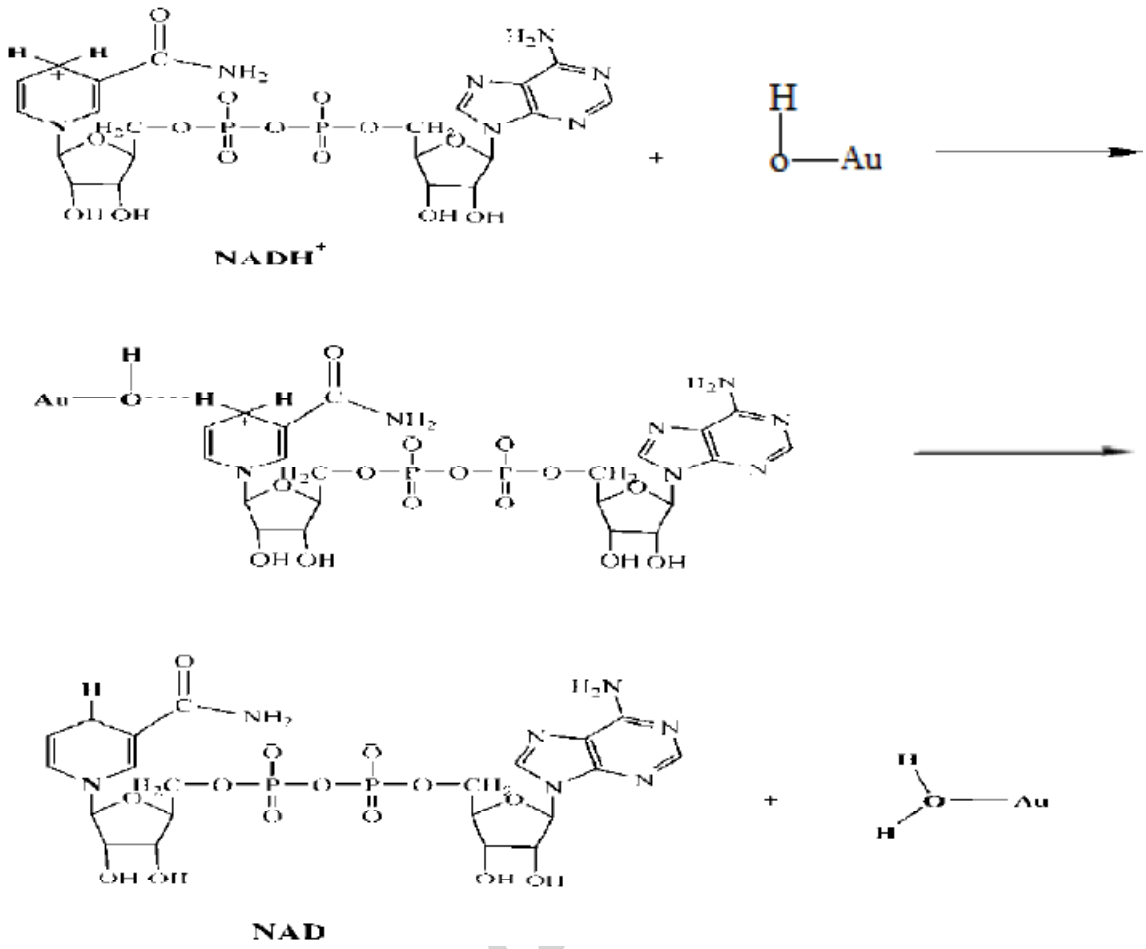

Scheme 1

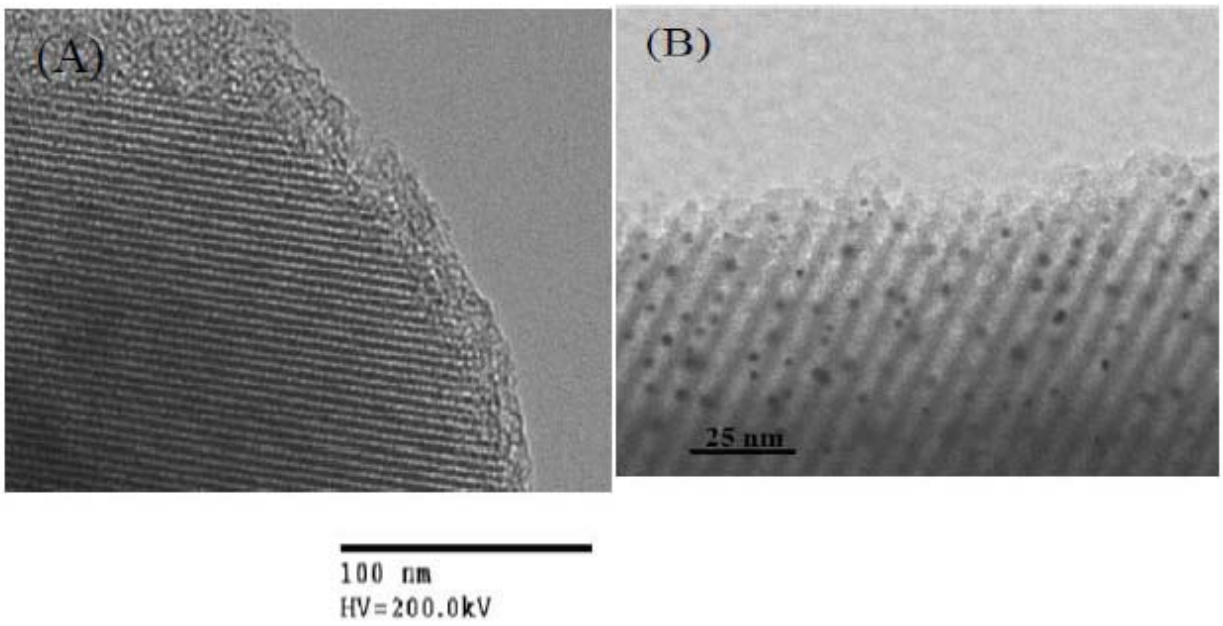

Fig. 1

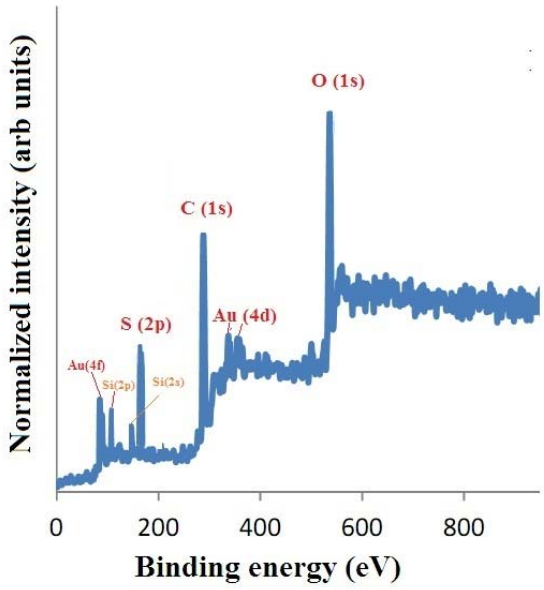

Fig. 2

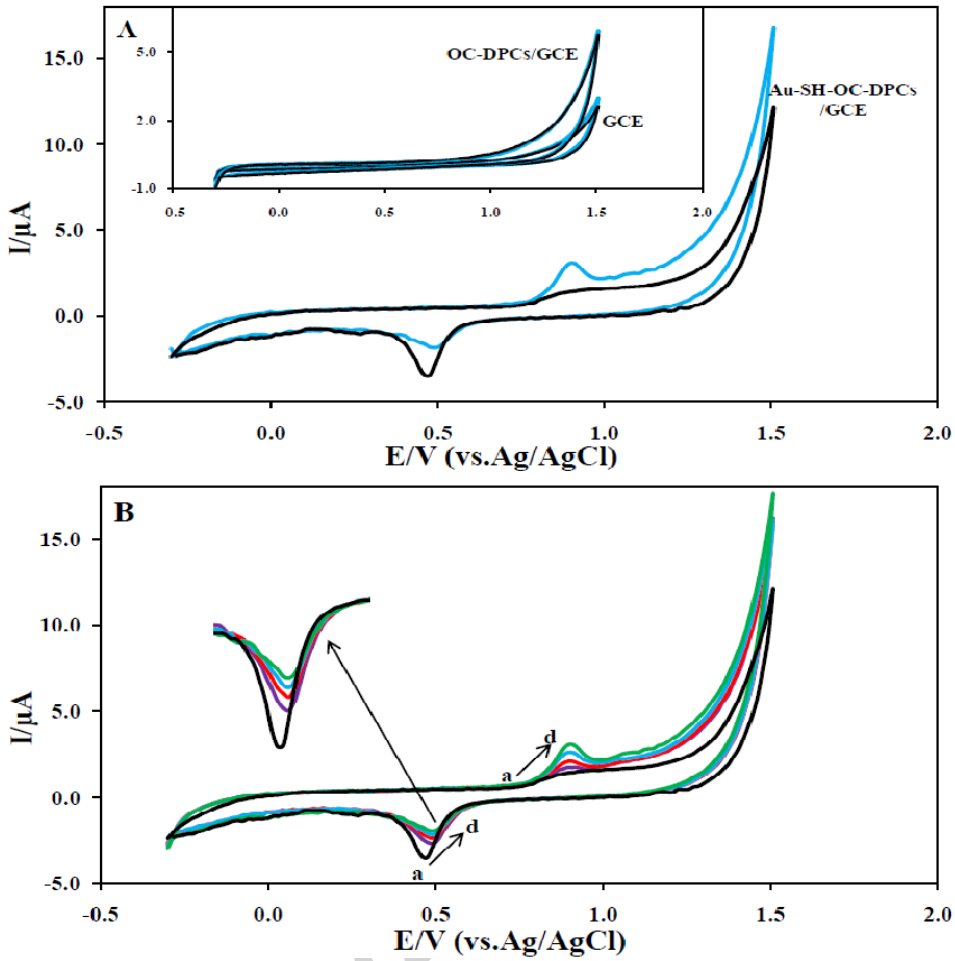

Fig. 3

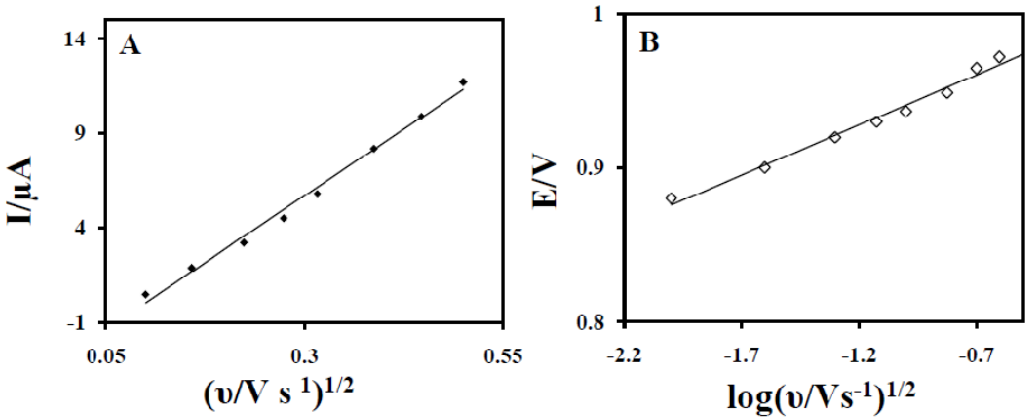

Fig. 4

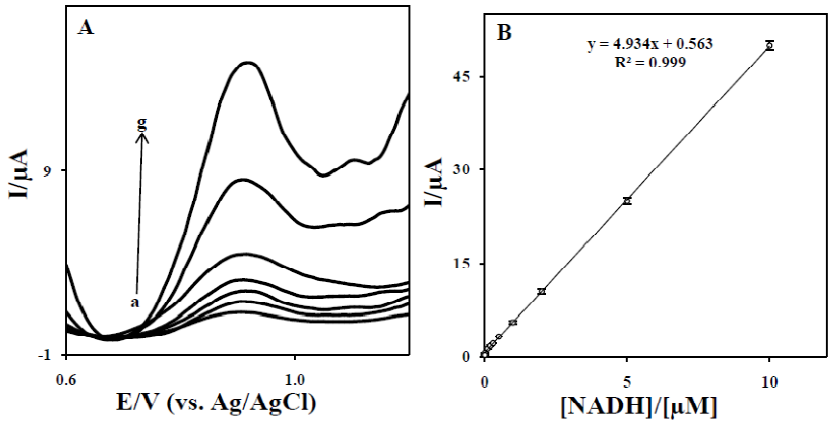

Fig.5

Highlights

► The Ordered carbohydrate-derived porous carbons immobilized gold nanoparticles (Au-SH-OC-DPCs) as a new electrocatalyst.
► The Au-SH-OC-DPCs as a new sensor for the electrooxidation of NADH.
► The detection limit of 1.0 nM and linear concentration range of 5.0 nM–10 μM for analysis of NADH at Au-SH-OC-DPCs.